

# Diffuse Optical Tomography: Image Reconstruction and Verification

Mohammad Ali Ansari, Mohsen Erfanzadeh, Zeinab Hosseini, Ezzedin Mohajerani

Laser and Plasma Research Institute, Shahid Beheshti University, G.C., Tehran, Iran

## Abstract:

**Introduction:** In this study, we intend to use diffuse optical Tomography (DOT) as a non-invasive, safe and low cost technique that can be considered as a functional imaging method and mention the importance of image reconstruction in accuracy and procession of image. One of the most important and fastest methods in image reconstruction is the boundary element method (BEM). This method is introduced and employed in our works.

**Method:** Generally, to image a biological tissue we must obtain its optical properties. In order to reach this goal we benefit from diffusion equation because tissue is highly scattering medium. Diffusion equation is solved by boundary element equation (BEM) in our research. First, we assume a double layer phantom with different scattering and absorption coefficients to simulate and verify procession and accuracy of image reconstruction by BEM. Light absorption can be affected by volume fraction of blood in skin. For a specific skin species the volume fraction is calculated and then the results are compared with the reconstructed values obtained by BEM. Since the depth of tissue is important in light absorption a two layer phantom with known values is made and the depths of layers are reconstructed by BEM then they are compared with the expected values. A homogenous phantom with known scattering and absorption coefficients was made and then these coefficients were reconstructed by BEM. Finally, an inhomogeneous phantom (phantom with defect) whose defect was in a known position was made and the absorption and scattering coefficients were reconstructed and compared with real values.

**Results:** Comparison between real or simulated values and reconstructed values of scattering and absorption coefficients, volume fraction of blood and thickness of phantom layers by BEM shows maximum errors of 24%, 7% and 35%, respectively.

**Conclusion:** Comparison between BEM data and real or simulated values shows an acceptable agreement. Consequently, we can rely on BEM as a beneficial method in diffuse optical tomography image reconstruction.

**Keyword:** optical tomography; phantom; laser.

---

Please cite this article as follows:

Ansari MA, Erfanzadeh M, Hosseini Z, Mohajerani E. Diffuse Optical Tomography: Image Reconstruction and Verification. *J Lasers Med Sci* 2014;5(1):13-8

---

**Corresponding Author:** Mohammad Ali Ansari, PhD; Laser and Plasma Research Institute, Shahid Beheshti University, Tehran, Iran; Tel: +98-2129904014; Fax: +98-2122431775; Email: m\_ansari@sbu.ac.ir

## Introduction

The diffuse optical tomography (DOT) is a new modality for biomedical imaging<sup>1-3</sup>. This technique has been applied for oncology and brain imaging. Optical mammography is a new application of DOT<sup>4-6</sup>. DOT is a

non-invasive and safe method that can be considered as a functional imaging method<sup>3</sup>. DOT, which is compared with the other modalities in Table 1, is currently emerging as a promising new addition to medical imaging<sup>6</sup>.

The image reconstruction algorithm is a critical problem in DOT. The accuracy and precision of diffuse optical

**Table 1.** Comparison of various medical imaging methods <sup>6</sup>

Characteristics	X-Ray Imaging	Ultra-sonography	MRI	DOT
Soft-tissue contrast	Poor	Good	Excellent	Excellent
Spatial resolution	Excellent	Good	Good	Good
Maximum imaging depth	Excellent	Good	Excellent	Good
Function	None	Good	Excellent	Excellent
Nonionizing radiation	No	Yes	Yes	Yes
Data acquisition	Fast	Fast	Slow	Fast
Cost	Low	Low	High	Low

imaging is related to the accuracy of image reconstruction. Hence, the design of an efficient algorithm for image reconstruction is of great importance. Dehgani et al. in 2009 made a new formalism for image reconstruction based on finite element method <sup>4</sup>. The capability of this formalism has been demonstrated through 2D and 3D examples that allow single wavelength, as well as multi-wavelength spectral modeling and image reconstruction. In 2010, Durduran reviewed the theoretical basis for near-infrared or diffuse optical spectroscopy, and also the basic elements of diffuse optical tomography for brain and breast functional imaging<sup>5</sup>. Lee in 2011 presented a review about the concept of diffuse optical tomography, its current clinical applications and its future outlook. A detailed theory of how to model the propagation of photons in highly scattering media and how to reconstruct 3D images out of a finite number of surface measurements is out of the scope of this paper, although a few basic equations and remarks are given in the next section <sup>6</sup>.

Most presented algorithms for image reconstruction are based on finite element method <sup>1, 4</sup>. In recent years, to study the propagation of photon in tissue, a new fast method based on boundary element method (BEM) has been introduced. The ability of BEM to study propagation of photon inside biological tissues has been evaluated. In previous studies, we applied this method to simulate the photon penetration inside biological tissues <sup>7</sup>.

In a previous study<sup>8</sup> we presented a low cost diffuse optical tomography and the propagation of near infrared (NIR) laser inside phantom was studied by this imaging setup. The presented device is capable of providing correct data of diffused light. It was also capable of detecting lesions inside the phantoms. In this study, however, we want to verify the ability of this device to detect the location of defects. First, the algorithm of image reconstruction is presented, and then the accuracy of this algorithm is verified. To verify this algorithm, the results obtained by image reconstruction are compared

with expected value of optical properties of phantom. The optical properties of phantom are similar to breast tissue.

Other diffuse optical tomography devices presented in the literature usually apply different sources, e.g. light of a laser diode is separated by an optical switching instrument and is coupled to several fiber optics <sup>2, 9</sup>. This multi-source scheme has some advantages but requires extra computational procedure such as calibration methods that raise the expense of this optical tomography. Therefore, in this study, the phantom is illuminated by a single source, and the reflectance on surface of the phantom is collected by an optical fiber; the collected signals are applied to determine the diameter and depth of tumors. The accuracy of this method is explored by comparing the reconstructed data with actual data.

## Methods

### 1. Image Reconstruction

The propagation of light in biological tissue can be modeled by diffusion equation<sup>10</sup>:

$$-\nabla \cdot D(\vec{r}) \nabla \phi(\vec{r}, \omega) + \left( a(\vec{r}) + \frac{i\omega}{c} \right) \phi(\vec{r}, \omega) = S(\vec{r}, \omega) \quad (1)$$

Here  $\vec{r}$  denotes position,  $\phi(\vec{r}, \omega)$  is the fluence rate defined as the energy flow per unit area per unit time. The anisotropic factor  $g$ , which is defined as,  $\langle \cos \theta \rangle$  has a value between  $-1$  and  $1$ . A value of zero indicates isotropic scattering, and a value close to unity indicates dominantly forward scattering. For most biological tissues,  $g$  is  $\sim 0.9$  <sup>10</sup>.  $S(\vec{r})$  is the isotropic source term at position  $\vec{r}$ . In this study the pump source is continuous; therefore the diffusion equation is applied in the stationary state.  $D(\vec{r})$  is referred to as the diffusion coefficient <sup>11</sup>:

$$D(\vec{r}) = \frac{1}{3(a(\vec{r}) + \sigma'(\vec{r}))} \quad (2)$$

Where,  $a(\vec{r})$  and  $\sigma' = \sigma(1 - g)$  are absorption and reduced scattering coefficients, respectively.

The diffusion equation can be solved by boundary element method (BEM). In this method, the differential equation is converted to an integral equation called the boundary integral method (BIM) and then this integral equation is solved by boundary element method (BEM)<sup>12</sup>. Our results have indicated that the computational time of BIM is less than finite-element methods (FEM) and Monte Carlo methods <sup>12-13</sup>. Usually the solution of the diffusion equation is called the forward method. In this study, the process of image reconstruction is based on the

BIM forward method for solving the diffusion equation for imaging domains. The reconstruction process solves an inverse problem to determine the optical properties of the tissue or the location of the in-homogeneous defect. The image reconstruction is achieved through an iterative procedure where an objective function consisting of the difference between the measured and the modeled data is minimized. In our case, the least-square functional to be minimized is<sup>14</sup>:

$$A^2 = \sum_{j=1}^m (\varphi_j^{\text{measured}} - \varphi_j^{\text{cal}})^2 \quad (3)$$

Where  $\varphi_j^{\text{measured}}$  and  $\varphi_j^{\text{cal}}$  are the measured and calculated fluences at the measurement point  $j$ , respectively.  $m$  is the total number of measurements. By using the least square criteria, the following nonlinear system of equations is achieved:

$$\begin{aligned} \frac{\partial A^2}{\partial \alpha_1} &\Rightarrow -\sum_{j=1}^m (\varphi_j^{\text{measured}} - \varphi_j^{\text{cal}}) \frac{\partial \varphi_j^{\text{cal}}}{\partial \alpha_1} = 0 \\ \frac{\partial A^2}{\partial \alpha_2} &\Rightarrow -\sum_{j=1}^m (\varphi_j^{\text{measured}} - \varphi_j^{\text{cal}}) \frac{\partial \varphi_j^{\text{cal}}}{\partial \alpha_2} = 0 \\ &\vdots \end{aligned} \quad (4)$$

$$\frac{\partial A^2}{\partial \alpha_{2n}} \Rightarrow -\sum_{j=1}^m (\varphi_j^{\text{measured}} - \varphi_j^{\text{cal}}) \frac{\partial \varphi_j^{\text{cal}}}{\partial \alpha_{2n}} = 0$$

Here the total number of  $a$  or  $D$  parameter is denoted by  $n$ . Also,  $\alpha$  expresses  $a$  or  $D$ . We define a vector:

$$B = (b_1, b_2, \dots, b_{2n})^T \quad (5)$$

in which  $b_i$  ( $i=1,2,\dots,2n$ ) denotes the left-hand side of each equation in Equation (4). By applying Newton's method, we have<sup>15</sup>:

$$\alpha_n = \alpha_{n-1} - G^{-1}B \quad (6)$$

where  $G$  (which is updated by  $\alpha$ ) is given by:

$$G = \begin{bmatrix} \frac{\partial b_1}{\partial \alpha_1} & \frac{\partial b_1}{\partial \alpha_2} & \dots & \frac{\partial b_1}{\partial \alpha_{2n}} \\ \frac{\partial b_2}{\partial \alpha_1} & \frac{\partial b_2}{\partial \alpha_2} & \dots & \frac{\partial b_2}{\partial \alpha_{2n}} \\ \vdots & \vdots & \ddots & \vdots \\ \frac{\partial b_{2n}}{\partial \alpha_1} & \frac{\partial b_{2n}}{\partial \alpha_2} & \dots & \frac{\partial b_{2n}}{\partial \alpha_{2n}} \end{bmatrix} \quad (7)$$

We define  $\Delta\alpha = \alpha_n - \alpha_{n-1}$ , so

$$G\Delta\alpha = -B \quad (8)$$

we can show that:

$$-B = J^T C \quad (9)$$

Where  $C$  is the data vector and it is given by:

$$C = (\varphi_1^{\text{measured}} - \varphi_1^{\text{cal}}, \varphi_2^{\text{measured}} - \varphi_2^{\text{cal}}, \dots, \varphi_m^{\text{measured}} - \varphi_m^{\text{cal}})^T \quad (10)$$

and  $J$  is the Jacobian matrix which is given by:

$$J = \begin{bmatrix} \frac{\partial \varphi_1}{\partial \alpha_1} & \frac{\partial \varphi_1}{\partial \alpha_2} & \dots & \frac{\partial \varphi_1}{\partial \alpha_{2n}} \\ \frac{\partial \varphi_2}{\partial \alpha_1} & \frac{\partial \varphi_2}{\partial \alpha_2} & \dots & \frac{\partial \varphi_2}{\partial \alpha_{2n}} \\ \vdots & \vdots & \ddots & \vdots \\ \frac{\partial \varphi_{2n}}{\partial \alpha_1} & \frac{\partial \varphi_{2n}}{\partial \alpha_2} & \dots & \frac{\partial \varphi_{2n}}{\partial \alpha_{2n}} \end{bmatrix} \quad (11)$$

One can see that the Jacobian matrix can be shown as

$$G = J^T J \quad (12)$$

Equation (8) is the basic equation of the inverse problem. By Taylor's expansion method and some mathematics, the following equation is derived<sup>16</sup>:

$$\partial\alpha = [J^T J + \eta I]^{-1} J^T C \quad (13)$$

$\eta$  is the regularization parameter selected based on phantom experiments.  $I$  is the unit matrix. Equation (11) can be iteratively solved to obtain the update in optical properties minimizing the difference between the calculated and measured data as indicated in equation (3). We implemented Equation (8) in order to perform iterative reconstruction for the optical properties based on a stopping criterion of a change in projection error given by the functional in equation (5) of less than 5% between following iterations.

## 2. Construction of Phantom and Experimental setup

Phantoms used in current study are made from Intralipid, as the scattering agent, Indian ink, as the absorber agent, and agarose as the base compound (agarose is transparent for NIR). The combination of Intralipid and Indian ink was diluted by distilled water in order to obtain necessary absorbing and scattering properties. These phantoms must represent the optical properties of breast tissue. The fabrication and control methods are based on reported methods in references number<sup>16-17</sup>. The scattering coefficient and anisotropic factor of 10% Intralipid can be achieved by the following equations<sup>7</sup>:

$$\sigma = 2.54 \times 10^9 \times \lambda^{-2.4}$$

$$g = 1.1 - 0.58 \times 10^{-3} \times \lambda \tag{13}$$

where,  $\lambda$  is the wavelength of light in nanometer and  $\sigma$  is the scattering coefficient ( $\text{cm}^{-1}$ ). Based on Equation (13), the scattering coefficient of Intralipid for  $\lambda = 780 \text{ m}$  is  $290.94 \text{ cm}^{-1}$ , in order to control the reduced scattering coefficient and absorption coefficient, we use the titration relation:  $C_{before} \times V_{before} = C_{after} \times V_{after}$ , where C is concentration and V is volume. Therefore, the reduced scattering and absorption coefficient can be controlled by these relations:

$$\sigma'_{before} \times V_{before} + \sigma'_{intralipid} \times V_{intralipid} = \sigma'_{after} \times V_{after}$$

$$a_{before} \times V_{before} + a_{intralipid} \times V_{intralipid} = a_{after} \times V_{after} \tag{14}$$

After the characterization of Intralipid and Indian ink, phantoms with optical properties close to healthy breast tissue were constructed<sup>17</sup>. In addition, phantoms in which cylindrical defects were placed inside were constructed. These phantoms cylinders with optical properties close to malignant breast tissue were placed inside the normal phantoms in different positions<sup>18</sup>. Details of the diffuse tomography device are reported in previous study<sup>8</sup>. The wavelength of laser Light is 780 nm. Light is brought to the phantom from a laser diode (WSTech, UT5-50G-780) by an optical fiber (Ocean Optics- QP-400-2-VIS/NIR).

### Simulation and Experimental Results

To verify the precision and accuracy of image reconstruction method, a double layer phantom is assumed. The optical properties of this phantom can be achieved by image reconstruction method. The precision and accuracy of image reconstruction method can be evaluated by comparison between the real and reconstructed values of optical properties. Tables 2-3 illustrates the precession of image reconstruction method. The maximum error in Table 1 and Table 2 are less than 23% and 4%, respectively.

The double layer model can be applied for skin. The tissue of skin can be modelled by a two layers tissue,

**Table 2.** Reconstructed value of absorption coefficient of first layer. The thickness of first layer is 1.0 mm.

Expected Value of Absorption Coefficient ( $\text{mm}^{-1}$ )	Reconstructed value of Absorption Coefficient ( $\text{mm}^{-1}$ )	% Error
$5.01 \times 10^{-2}$	$4.25 \times 10^{-2}$	15
$11.34 \times 10^{-2}$	$87.00 \times 10^{-2}$	23
$18.00 \times 10^{-2}$	$15.50 \times 10^{-2}$	14

**Table 3.** Reconstructed value of scattering coefficient of second layer. The thickness of first layer is 1.0 mm.

Expected Values of Scattering Coefficient ( $\text{mm}^{-1}$ )	Reconstructed Value of Scattering Coefficient ( $\text{mm}^{-1}$ )	% Error
10.00	10.15	1.5
20.00	19.3	3.5
25.00	24.00	4

epidermis and dermis, illuminated by a flat-top laser beam. The thickness of the former layer is assumed to be finite, while the thickness of the second layer is assumed infinite. The subcutaneous fat is not considered due to its negligible effects in NIR region<sup>16, 18</sup>. We have also assumed melanosome and blood vessel to be uniformly distributed in epidermis and dermis layers, respectively. The light absorption in skin depends on the volume fraction of melanosome and hemoglobin in epidermis and dermis. The reconstructed values of volume fraction of blood are calculated by the image reconstruction method (Table 4).

Previous tables depict that the presented reconstruction method can be applied to calculate the optical properties of biological tissues such as skin. In optical imaging, the depth of lesion inside tissue is important. To verify the ability of the reconstruction method, the thickness of first layer (two-layer phantom) changes from 0.5 mm to 1.5 mm, and the thickness of this layer is reconstructed as shown in Table 5.

The presented results in Tables 2-5 illustrate the image reconstructed method based on BEM can be applied with sufficient accuracy. But, the accuracy of this method decreases for larger value of thickness. That is because, absorption of light increases for larger thickness and therefore, the intensity of reflectance decreases. Figure 1

**Table 4.** The reconstructed value of volume fraction of blood in dermis.

Expected Value of Volume Fraction of Blood	Reconstructed Value of volume Fraction of Blood	%Error
0.15	0.14	7
0.20	0.19	5
0.32	0.31	4

**Table 5.** The reconstructed value of thickness of first layer.

Expected Value of Thickness	Reconstructed Value of Thickness	% Error
0.50	0.47	6
1.0	0.65	35
1.10	1.08	1.8
1.20	1.04	13
1.50	1.80	20

depicts the penetration of laser light in the two-layer phantom. One can see that for larger values of depth, the fluence decreases.

The presented data depict that BEM can be applied for image reconstruction. To study the accuracy of this reverse model, a homogeneous phantom with diameter of 3.6 cm was constructed. The absorption and reduced scattering coefficient of this phantom are  $0.074 \text{ cm}^{-1}$  and  $1.14 \text{ cm}^{-1}$ , respectively. The measured intensities around the phantom,  $\varphi_j^{\text{measured}}$ , are applied in image reconstruction method as the input data. The reconstructed values of absorption and scattering coefficient have been estimated as  $0.09 \text{ cm}^{-1}$  and  $1.2 \text{ cm}^{-1}$ , respectively; the overall error is less than 14%.

Figure 2 depicts the measured intensity around the

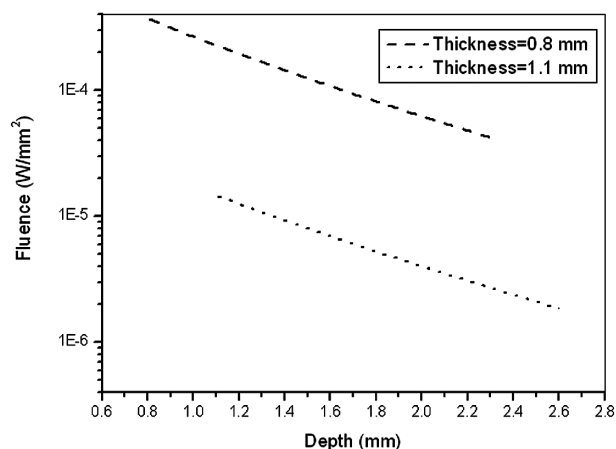


**Figure 1.** The penetration of laser light ( $\lambda = 780 \text{ nm}$ ) for two different value of thickness of first layer.

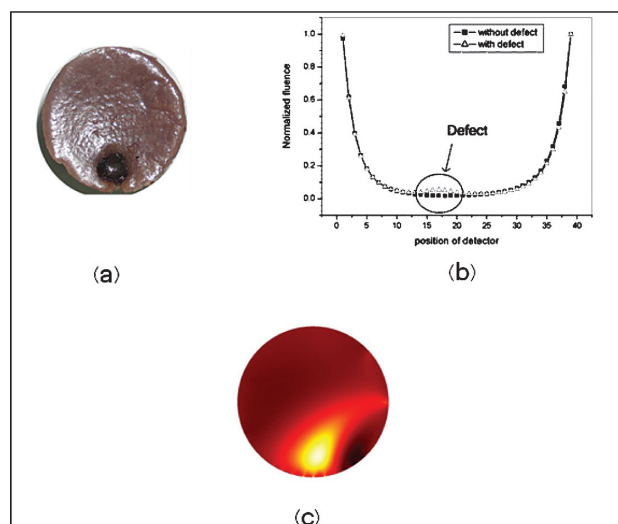


**Figure 2.** The Reconstructed image of an in-homogeneous phantom. The image of phantom (a) and the comparison between measured intensities around homogeneous and in-homogeneous phantom (b), and the position of defect can be seen in (c).

homogeneous and in-homogeneous (phantom with a defect). The value of diameter of defect is 0.7 cm, and the absorption and reduced scattering coefficient of this phantom are  $0.15 \text{ cm}^{-1}$  and  $1.92 \text{ cm}^{-1}$ , respectively. The position of defect can be seen in Figure 2. The reconstructed values of absorption and scattering coefficient of this defect have been estimated as  $0.16 \text{ cm}^{-1}$  and  $2.2 \text{ cm}^{-1}$ , respectively; the overall error is less than 15%.

## Conclusion

Data comparison between simulated and reconstructed scattering and absorption coefficients in two-layer phantoms shows a good procession and accuracy. We can find volume fraction of blood tissue by light absorption via BEM with a suitable procession and accuracy. Tissue depth is an important parameter in diffuse optical tomography which BEM has good ability to reconstruct. Nevertheless, in thick tissue layers its accuracy decrease due to the small value of data received from reflectance. Accuracy verification of BEM for a homogenous phantom by comparing measured intensities with BEM reconstruction data was performed and an acceptable value of 14% error was achieved. The inhomogeneous phantom was used to simulate tumorous tissue experiment in which comparison between real scattering and absorption coefficients with reconstructed data by BEM has a hopeful correlation.

## Acknowledgement

This research was supported by Laser Application in Medical Sciences Research Center (Shahid Beheshti University of Medical Science) by the grant number L/M/2193. The authors would like to acknowledge the contribution of Mr. Mohsen Shojaeifar for very helpful discussions.

## References

1. Choe R, Corlu A, Lee K, Durduran T, Konecky SD, Grosicka-Koptyra M. Diffuse optical tomography of breast cancer during neoadjuvant chemotherapy: A case study with comparison to MRI. *Med Phys* 2005;32(4):1128-39.
2. Tromberg BJ, Poguea BW, Paulsen KD, Yodh AG, Boas DA, Cerussi AE. Assessing the future of diffuse optical imaging technologies for breast cancer management. *Med Phys* 2008;35(6):2443-51.
3. Izzetoglu K, Bunce S, Onaral B, Pourrezaei K, Chance B. Functional Optical Brain Imaging Using Near-Infrared during

- Cognitive Tasks. *Int J Hum Comput Interact* 2004;17(2):211-27.
4. Dehghani H, Eames ME, Yalavarthy PK, Davis SC, Srinivasan S, Carpenter CM, et al. Near infrared optical tomography using NIRFAST: Algorithm for numerical model and image reconstruction. *Commun Numer Methods Eng* 2008;25:711-32.
  5. Durduran T, Choe R, Baker WB, Yodh AG. Diffuse optics for tissue monitoring and tomography. *Rep Prog Phys* 2010;73(7):076701.
  6. Wang LV, Wu H, Biomedical optics: Principles and imaging. Wiley-Interscience 2007.
  7. Ansari MA, Alikhani S, Mohajerani E, Massudi R. The numerical and experimental study of photon diffusion inside biological tissue using boundary integral method. *Opt Commun* 2012;285(5) :851-5.
  8. Erfanzadeh M, Alikhani S, Ansari MA, Mohajerani E. A Low-Cost Method for Optical Tomography: *J Lasers Med Sci* 2011; 3(3):102-8.
  9. Welch AJ, Gemert MVC. *Optical-Response of Laser-Irradiated Tissue*. First ed. Springer 1995.
  10. Ghosh N, Mohanty SK, Majumder SK, Gupta PK. Measurement of Optical Transport Properties of Normal and Malignant Human Breast Tissue. *Appl Opt* 2001; 40(1):176.
  11. Sikora J, Zacharopoulos A, Douiri A, Schweiger M, Horesh L, Arridge SR, et al. Diffuse photon propagation in multilayered geometries. *Phys Med Biology* 2006; 51:497-516.
  12. Ansari MA, Massudi R. Study of short-pulse laser propagation in biological tissue by means of the boundary element method. *Lasers Med Sci* 2011; 26(4):503-8.
  13. Ansari MA, Massudi R. Boundary integral method for simulating laser short-pulse penetration into biological tissues. *J Biomed Opt* 2010; 15(6):065009.
  14. Jiang H. *Diffuse Optical Tomography*, CRC press 2007.
  15. Kumar D, Srinivasan R, Singh M. Optical characterization of mammalian tissues by laser reflectometry and Monte Carlo simulation. *Med Eng Phys* 2004;26(5):363-9.
  16. Choe R. Diffuse optical tomography and spectroscopy of breast cancer and fetal brain. p. 83. Thesis of doctor of philosophy, Department of Physics and Astronomy University of Pennsylvania 2005.
  17. Ansari MA, Erfanzadeh M, Alikhani S, Mohajerani E. The study of effect of mechanical pressure on determination of position and size of tumor in biological phantoms. *Appl Opt* 2013;52(12):2739-49.
  18. Mordon SR, Wassmer B, Reynaud JP, Zemmouri J. Mathematical modeling of laser lypolysis. *Biomed Eng Online* 2007;7:1-13.